

Manuscript version: Author's Accepted Manuscript

The version presented in WRAP is the author's accepted manuscript and may differ from the published version or Version of Record.

Persistent WRAP URL:

<http://wrap.warwick.ac.uk/130171>

How to cite:

Please refer to published version for the most recent bibliographic citation information. If a published version is known of, the repository item page linked to above, will contain details on accessing it.

Copyright and reuse:

The Warwick Research Archive Portal (WRAP) makes this work by researchers of the University of Warwick available open access under the following conditions.

Copyright © and all moral rights to the version of the paper presented here belong to the individual author(s) and/or other copyright owners. To the extent reasonable and practicable the material made available in WRAP has been checked for eligibility before being made available.

Copies of full items can be used for personal research or study, educational, or not-for-profit purposes without prior permission or charge. Provided that the authors, title and full bibliographic details are credited, a hyperlink and/or URL is given for the original metadata page and the content is not changed in any way.

Publisher's statement:

Please refer to the repository item page, publisher's statement section, for further information.

For more information, please contact the WRAP Team at: wrap@warwick.ac.uk.

ARTICLE

Effect of the addition of salt to Pickering emulsion polymerizations using polymeric nanogels as stabilizer

Andrea Lotierzo,^a Shane P. Meaney,^b and Stefan A. F. Bon*^a

Received 00th January 20xx,
Accepted 00th January 20xx

DOI: 10.1039/x0xx00000x

Nanogels made from crosslinked block copolymer micelles are used as stabilizers in the Pickering emulsion polymerization of styrene. The effect of the addition of salt, *i.e.* NaCl, on the emulsion polymerization is studied. It is shown that an increase in ionic strength of the dispersing medium in these polymerizations led to the formation of latexes of larger diameters. Along with an increase in size, the morphology of these polymer colloids changed from Janus to patchy with an increase in number of nanogels adsorbed on the polymer surface, as a function of the salt concentration in water. In particular, at the highest tested ionic strength, ca. 25 mM, fully armored polymeric particles surrounded by a dense layer of adsorbed stabilizing nanogels were formed. Kinetic studies carried out at varying NaCl concentrations suggested that particle formation in the reaction followed a combination of a coagulative nucleation mechanism, characterized by a clustering process of Janus precursors to form bigger aggregates, and droplet nucleation. Preliminary film formation studies on latexes made with *n*-butyl acrylate as comonomer indicated the potential of this technique for the production of coherent polymer films which included a substructure of functional nanogels.

Introduction

Waterborne polymer dispersions find applications in a variety of fields, including the coating,¹ pharmaceutical² and adhesive³ industries, in the production of nanocomposite materials⁴ or plastics and rubbers,⁵ and even as promising candidates for the design of future batteries⁶ and solar cells.⁷ In the past few decades, synthetic methods were developed to design polymer particles of different sizes,⁸ morphologies,⁹ and functionalities.¹⁰ A common way of synthesizing waterborne polymer colloids is *via* emulsion polymerization. In a standard emulsion polymerization process, a water-insoluble monomer, a surface-active agent and an initiator are added to water. Upon radical formation in the water phase, for instance by thermal decomposition of the initiator, a dispersion of polymer latex particles is obtained. The name emulsion polymerization erroneously suggests the direct transformation of the monomer droplets into polymer particles.¹¹ The role of the molecular surfactants is to aid particle nucleation by means of radical entry into existing micelles, and to provide colloidal stability of the growing polymer latex particles. Surfactant-free systems were also developed in the 1970s in a way to avoid tedious purification processes or detrimental side-effects resulted from the presence of surface-active agents in specific applications.¹² Even in this case, nucleation of monomer droplets in water is an

unlikely event¹³ and particle formation takes place in the continuous phase *via* homogeneous nucleation.¹¹

By 2010 the concept of Pickering emulsion polymerization was established, in which the role of molecular surfactants was fulfilled by nanoparticles, serving as Pickering stabilizers, instead. Examples include silica nano-sols,^{14–17} clay nanodiscs,^{18–20} cerium oxide nano-particles,²¹ polymeric Janus particles,^{22,23} graphene oxide sheets,²⁴ and cellulose nanocrystals.²⁵ Recently, we showed that crosslinked polymer nanoparticles, or nanogels, can be used as a class of Pickering stabilizers to synthesize anisotropic polymer colloids of Janus and patchy particle morphology.²⁶

In this paper, we would like to investigate the role of inert electrolyte, or salt, on the Pickering emulsion polymerization process in which nanogels are used as stabilizer. The addition of electrolytes has an impact on emulsion polymerization reactions from a mechanistic standpoint. Their role in standard and surfactant-free emulsion polymerization was investigated a few decades ago.^{8,12,27–32} Overall, previous research agreed that the progressive increase in ionic strength in the continuous phase results in larger polymer particles. This was attributed mostly to the formation of fewer stable particles during the nucleation step (Stage I of emulsion polymerization)³³ due to an increase in coagulative nucleation events between primary particles.^{8,12,29} It is clear that the increase in the obtained latex size is controllable up to a certain ionic strength, above which complete coagulation of the system is observed.²⁸ Mathematical treatment of the rate of coagulation of newly formed oligomers in Stage I clearly showed that the size of the first stable colloid formed is highly dependent on the ionic strength, as this affects directly the surface charge density and the electrostatic surface potential.⁸ Interestingly, an estimate of

^a Department of Chemistry, University of Warwick, Coventry CV4 7AL, U.K.

^b School of Chemistry, Monash University, Clayton 3800, Australia. Current address: Division of Enterprise, The University of New South Wales, Kensington 2052, Australia

* To whom all correspondence should be addressed: s.bon@warwick.ac.uk
Electronic Supplementary Information (ESI) available: [details of any supplementary information available should be included here]. See DOI: 10.1039/x0xx00000x

the time required for this controlled coagulation to happen was found to be in the timescale of few minutes (< 20 min) in the case of a 24h long reaction.^{8,34} Additionally, an increase in electrolyte concentration seemed to shorten the duration of Stage I (particle formation) and decrease the polymerization rate during Stage II (particle growth).^{27,28}

Whilst classical emulsion polymerization literature mostly focused on the regulation of particle size distribution, more recent work indicated that, especially in the presence of seed particles, electrolytes could be used to produce armored nanocomposite polymer colloids. For instance Thickett and Zetterlund showed that the variation of ionic strength in emulsion polymerizations of styrene conducted in the presence of graphene oxide (GO) nano-sheets could lead to the formation of inorganic-organic hybrid particles.²⁴ This behavior was attributed to the instability of GO at higher ionic strengths with the consequent enhanced likelihood of heterocoagulation with growing oligomers in the water phase. The inspiration for this work also came from other research, not strictly related to salt addition to emulsion polymerization reactions. These studies suggested that “complex” colloids could be synthesized by colloidal instability of smaller *stabilizers*, or seeds, coupled with good interaction with a *stabilized* phase. In previous work from Bon *et al.* Laponite clay disks were rendered unstable by dispersion of the clay in NaCl aq. solutions and, as a result, they behaved as Pickering stabilizers for oil-in-water mini-emulsions.^{35,36} Analogously, we previously showed that destabilization of SiO₂ by pH lowering in methyl methacrylate Pickering emulsion polymerization led to the formation of polymer latexes surrounded by a shell of silica particles.^{14,16,17}

In all the examples above, the destabilization of the Pickering nanosols originated from a compression of the diffusive double layer, with a consequent reduction of electrostatic repulsion.³⁷ This facilitated the synthesis of polymer particles armored with a layer of Pickering stabilizers. As described above, we recently showed that by using nanogels we can open up the particle morphology window away from fully armored structures into Janus and Patchy morphologies.²⁶ The objective of the work reported here is to explore the role of salt in regulating particle morphology.

Results and discussion

A series of Pickering emulsion polymerizations under batch conditions was carried out using styrene as monomer and nanogels made from crosslinked poly(methyl methacrylate-*co*-methacrylic acid)-*block*-poly(*n*-butyl methacrylate), P(MMA-MAA-*co*-PBMA, micelles. The effect of salt addition on the polymerization was investigated upon variation of electrolyte concentration, here NaCl, in the water phase. The nanogels were prepared as described previously.²⁶ Table 1 summarizes their key properties. The MMA/MAA molar ratio was 1.8/1.0, and the average degree of polymerization (*DP*) was 17 and 10 respectively for the first (hydrophilic) and second (hydrophobic) block. The diblock copolymer micelles were crosslinked using

trimethylolpropane trimethacrylate to yield the nanogels. An interesting feature of the nanogels is that they still have residual double bonds as confirmed by ¹H-NMR of a 1.0 wt% nanogel suspension in D₂O (Figure S1).

Table 1. Summary of some of the properties of the nanogels adopted in this work.

	$M_w / ^a \text{ kg mol}^{-1}$	$\mathcal{D} / ^a -$	$d_{\text{SAXS}} / ^b \text{ nm}$	$d_H / ^c \text{ nm}$	$Pdl / ^c -$
Nanogels	5.6	1.6	18	30	0.14

^a Weight average molecular weight (M_w) and polymer dispersity (\mathcal{D}) of the micellar unimers measured by size exclusion chromatography before crosslinking (DMF + 5 mM NH₄BF₄, PMMA narrow standards).

^b d_{SAXS} = diameter of the nanogel from SAXS measurements done at pH = 6.0 and 10 mg/ml. A spherical model was used in the fitting.

^c Hydrodynamic diameter (d_H) and polydispersity index (Pdl) measured by dynamic light scattering (DLS) at 5.0 mg/ml, pH = 8.5.

Charged colloidal particles are known to rely on the repulsion of the electrostatic fields surrounding them to maintain colloidal stability.³⁸ The degree of extension of the electrical double layer is typically associated to the so-called Debye-Hückel parameter κ (Equation 1).³⁷ Its reciprocal, κ^{-1} , also known as Debye Length, has units of length and is used as a measure for the thickness of the diffuse double layer.

$$(1.1) \quad \kappa = \left(\frac{e^2 N_A}{\epsilon k_B T} 2I \right)^{1/2} = \left(\frac{e^2 N_A}{\epsilon k_B T} \sum_{i=1}^n M_i z_i^2 \right)^{1/2}$$

where e is the elementary charge, N_A is the Avogadro number, k_B is the Boltzmann constant, T is the absolute temperature, I is the ionic strength, z_i is the charge of the i ion, M_i is its molar concentration and ϵ is the specific permittivity of the solvent.

A measure of colloidal stability in electrostatically stabilized particles is the so-called ζ -potential, which has a dependence on

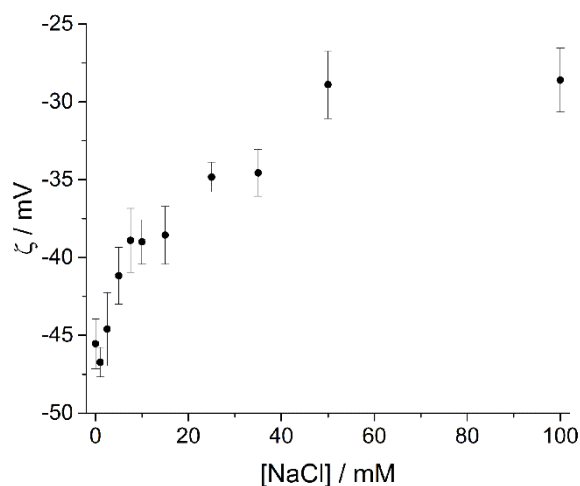


Figure 1. ζ -potential of a 1.0 wt% aq. dispersion of nanogels measured at different [NaCl] at 25°C and pH 8.8.

κ^{-1} ; its absolute value is reduced for higher electrolyte concentrations. This effect is demonstrated in Figure 1, in which the ζ -potential of an aqueous nanogel dispersion was measured at pH 8.8 as a function of NaCl concentration. ζ reached a value of *ca.* -29 mV at around [NaCl] = 50 mM. Despite the double layer compression, the nanogels were surprisingly stable over the whole range of [NaCl] tested, as also confirmed by dynamic light scattering measurements (DLS) (Figure S2). This is particularly interesting as in previous work from our group we observed that the formation of colloidal suprastructures (*i.e.*

patchy particles) was favored in a pH range where nanogel clustering was observed,²⁶ which is considerably different from what observed for ionic strength increase.

In a typical Pickering emulsion polymerization experiment an aqueous dispersion of nanogels (13.0 wt% aq. suspension) was diluted with aq. NaCl. The monomer-to-water ratio was approximately 0.1. Polymerizations were carried out at 75°C using potassium persulfate as initiator. The effect of NaCl

Table 2. Size, dispersity and coagulum formed in the nanogel-stabilized emulsion polymerizations of styrene conducted in the presence of NaCl.

[NaCl] / mM	κ^{-1} / ^a nm	DLS		CHDF ^b		Coagulum / ^c wt%
		d_H / nm	Pdl / -	D / nm	σ / nm	
0.0	8.7	91	0.016	89	10	-
1.0	6.4	93	0.021	89	12	-
2.5	4.9	107	0.050	97	25	-
5.0	3.8	158	0.086	138	49	-
7.5	3.2	262	0.080	269	96	1.7
10.0	2.8	505	0.184	462	146	2.0
15.0	2.3	642	0.186	599	146	22.0
25.0	1.8	963	0.243	-	-	42.6
18.9 ^d	1.6	586	0.064	-	-	4.0

^a Calculated using Equation 1 in reaction conditions: 75°C, [KPS] = 0.25 mM, total ionic strength (*I*) = 1.16 mM before NaCl addition.

^b Capillary hydrodynamic fractionation (CHDF) analysis; *D* is the weight average diameter and σ its standard deviation.

^c Calculated as the ratio of the solid content of the final latex (measured *via* freeze-drying) over the theoretical one assuming 100% monomer conversion.

^d Same total *I* as the reaction performed at [NaCl] = 25.0 mM but a higher initiator concentration was adopted; [KPS] = 2.50 mM.

addition on the emulsion polymerizations was tested by a series of reactions performed in 0.0 to 25.0 mM NaCl aq. solutions (Table 2).

In these experiments the pH was kept at a value of about 8.8 in order to have complete dissociation of the acid groups in the nanogel corona (degree of ionization of polymethacrylic acid at pH 8.8 is *ca.* 1).^{39,40} The amount of nanogels was kept constant across all the experiments at a weight ratio of 0.0285 wrt to

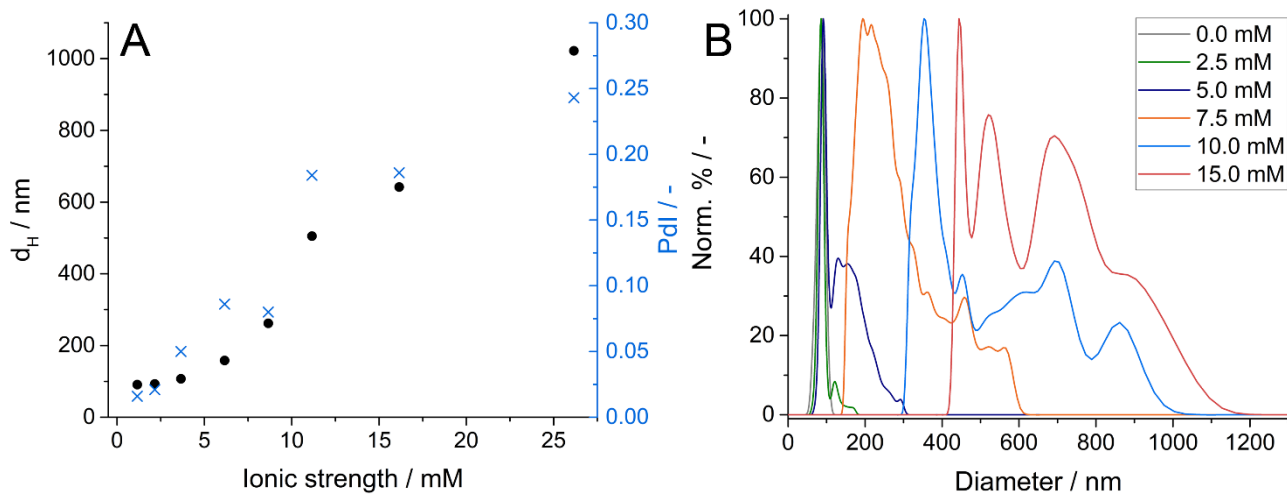


Figure 2. a) Variation of the particle hydrodynamic diameter (d_H) and dispersity (Pdl) with the system total ionic strength (added NaCl + base ionic strength) of the nanogel-stabilized styrene emulsion polymerizations. b) Capillary hydrodynamic fractionation (CHDF) fractograms displaying the normalized weight size distribution of the latexes produced at different [NaCl].

monomer. As can be seen from Table 2, the reactions performed at higher [NaCl] led to some limited coagulation, which for the highest two salt concentration was substantial. Whilst the formation of coagulum is not particularly problematic in laboratory scale experiments (~200 g), this must be tackled for instance before considering industrial applicability of the technique. All the isolated latexes after removal of the coagulum by filtration were stable over the course of few months after their synthesis. Even in the case of settling/sedimentation over a prolonged time, the particles could easily be re-dispersed upon gentle shaking of the latexes. As an attempt to reduce the amount of coagulum formed, we increased the initiator concentration 10-fold (Table 2, last entry). The coagulum formation in this case was indeed reduced down to 4 wt%. The reason for this is that the initiator derived sulfate end groups of the polymer chains, together with water soluble oligomers made *in situ*, aid the stabilization of the polymer latex. As expected, this also came with a decrease in average particle diameter and dispersity, as a larger number of latex particles are nucleated in a shorter period of time at higher initiator flux. A first estimate in terms of rate of nucleation can be given by the time necessary to form enough radicals to nucleate all the nanogel present (here not considering exit for simplicity of the discussion).¹⁷ At lower initiator concentration the time required to have equal number of radical produced (efficiency of radical capture, f , ~ 0.16)⁴¹ and number of nanogels = 435 seconds, whereas this number goes down to 135 seconds when ten times more initiator is adopted ($f = 0.05$).⁴¹

DLS analysis of the latexes showed that the salt addition had a dramatic effect on the hydrodynamic diameter (d_H) and dispersity (PdI) of the obtained particles (Figure 2A and Table 2). This confirmed what previously observed in the literature;

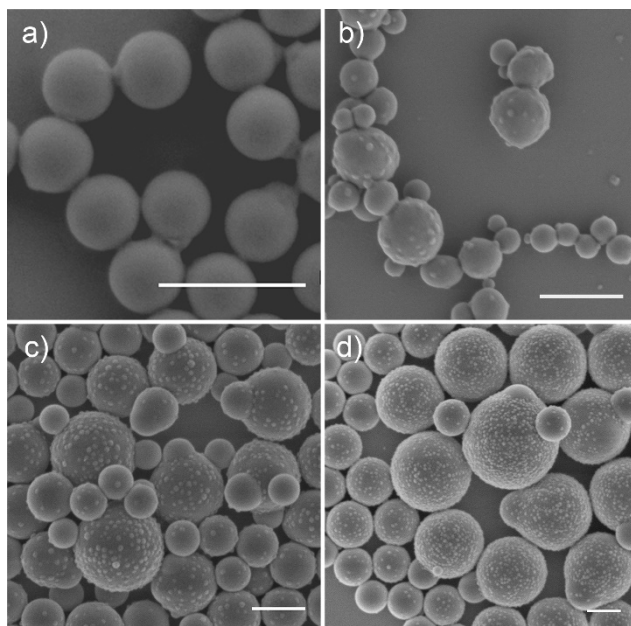


Figure 3. Emulsion polymerizations of styrene performed at pH 8.8 and using carboxylic acid functionalized nanogels as stabilizers. The reactions were conducted in the presence of a) 0.0 mM, b) 5.0 mM, c) 7.5 mM, d) 10.0 mM aq. NaCl as background electrolyte. [KPS] = 0.25 mM. Scale bars: 300 nm.

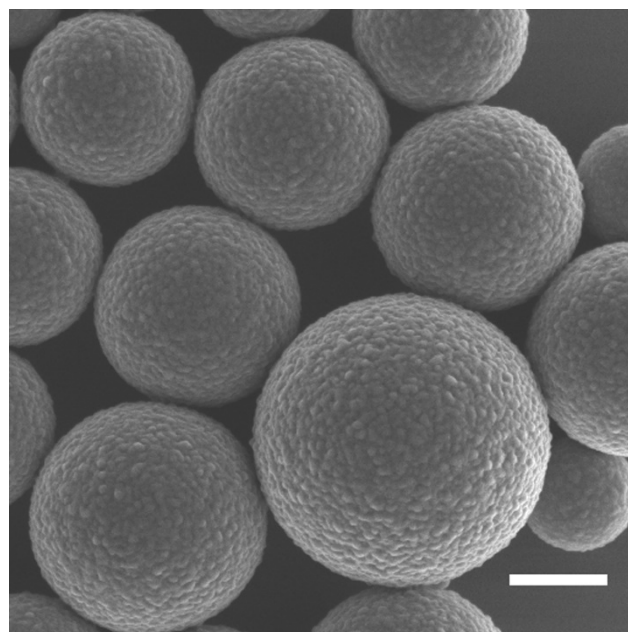


Figure 4. Emulsion polymerization conducted in the presence of 18.9 mM aq. NaCl as background electrolyte and [KPS] = 2.50 mM. Scale bar: 300 nm.

overall the addition of a background electrolyte to emulsion polymerizations produces bigger latex particles.^{8,12,27–32} However, the extent of the addition on the latex hydrodynamic diameter was interestingly much more pronounced than what previously observed,^{12,27,28} d_H varied from about 90 nm in absence of added electrolytes to almost 1000 nm when the reaction was carried out in 25.0 mM [NaCl]. The addition of salt seemed to have no effect on the final particle size for small additions of NaCl, *i.e.* 1.0 mM, after which a gradual increase of d_H with [NaCl] was observed up to about [NaCl] = 7.5 mM. At larger salt concentrations, a marked raise in size was observed, which then increased in the range 10.0 – 25.0 mM [NaCl], along with the dispersity of the latexes (Figure 2A and Table 2).

Given the dispersity of the samples obtained, capillary hydrodynamic fractionation (CHDF) was used to obtain a more statistical and visual representation of the particle size distribution. CHDF is a particle separation technique based on the following principle. When colloidal particles of different sizes are dispersed in a liquid medium and travel across a capillary on narrow dimension, typically 4–10 μm in diameter, they are separated and emerge in order of decreasing diameter.^{42–44} The fractionation is the result of different fluid velocities in the capillary caused by the formation of a parabolic flow profile.⁴⁵ Larger particles are drawn to the center of the capillary and hence elute quicker. CHDF overcomes the limitations of dynamic light scattering measurements of hiding or underestimating the presence of smaller colloids in polydisperse mixtures.³³ CHDF fractograms of the nanogel stabilized latexes are shown in Figure 2B whereas the latexes weight average diameters (D) and standard deviations (σ) are reported in Table 2.

Beside the effect of salt addition on the final particle size distribution of the obtained polymer latexes, we wanted to find out more about the particle morphology. The reason for this was that in a previous study we showed that when Pickering emulsion polymerizations of styrene were conducted in the presence of nanogels at progressively lower pH, hence decreasing the degree of ionization of methacrylic acid in the nanogel corona, patchy particles consisting of a poly(styrene) core surrounded by a controlled adsorbed number of nanogel patches were observed.²⁶

Scanning electron microscopy (SEM) analysis on the latexes obtained showed that variation in patch, *i.e.* nanogel, density on the surface of the particles could also be achieved upon addition of background electrolyte (Figure 3), albeit to less precision. When no additional electrolyte was added, Janus particles of narrow size distribution consisting of a polystyrene core bearing a single patch were obtained (Figure 3A). At 2.5 mM [NaCl], larger particles (*ca.* 130-190 nm) with more nanogels on their surface started to appear (Figure S3). These patchy particles progressively increased in number and size moving to 5.0 and 7.5 mM NaCl (Figures 3B and 3C). In the latter case, all the observed particles appeared to have multiple patches on their surface. This came with a noticeable raise in dispersity in both size and patch density, with the latter decreasing for smaller particles within the same sample. The addition of 10.0 mM of background electrolyte produced particles of much bigger sizes and with noticeable denser nanogel coverage on their surface (Figure 3D). This trend continued at even higher [NaCl] and in particular at 25.0 mM [NaCl] just one particle population of considerable dispersity was formed, characterized by a very dense layer of nanogels on their surface (Figure S4). These dense patched morphologies are in essence fully armored latex particles, resembling the structures obtained in Pickering emulsion polymerizations with inorganic stabilizers.¹⁴⁻²¹

As stated in Table 2, at high salt concentrations considerable amounts of coagulum were formed in first instance restricting the accessibility to fully armored structures. As indicated before, a higher initiator flux can be used to alleviate this. Fully armored latexes can then be obtained with minor coagulation issues (Figure 4).

After these initial observations a series of questions still remained unanswered regarding the patchy and armored particles formation mechanism and the origin of the broad dispersity of the particle size distribution. Additionally, for 5.0 mM \leq [NaCl] \leq 15.0 mM a portion of the more densely covered latexes were not perfectly spherical. The frequency of the presence of such latexes decreased by moving from 2.5 mM to 25.0 mM, with the latter consisting of only spherical latexes. In order to come to a better understanding of the process, some kinetic experiments were carried out on the reactions at 0.0, 7.5, 10.0 and 25.0 mM [NaCl]. Monomer conversion (X) vs. reaction time and d_H vs. X for these reactions are displayed in Figure 5. In order to discuss the data presented, the equation to

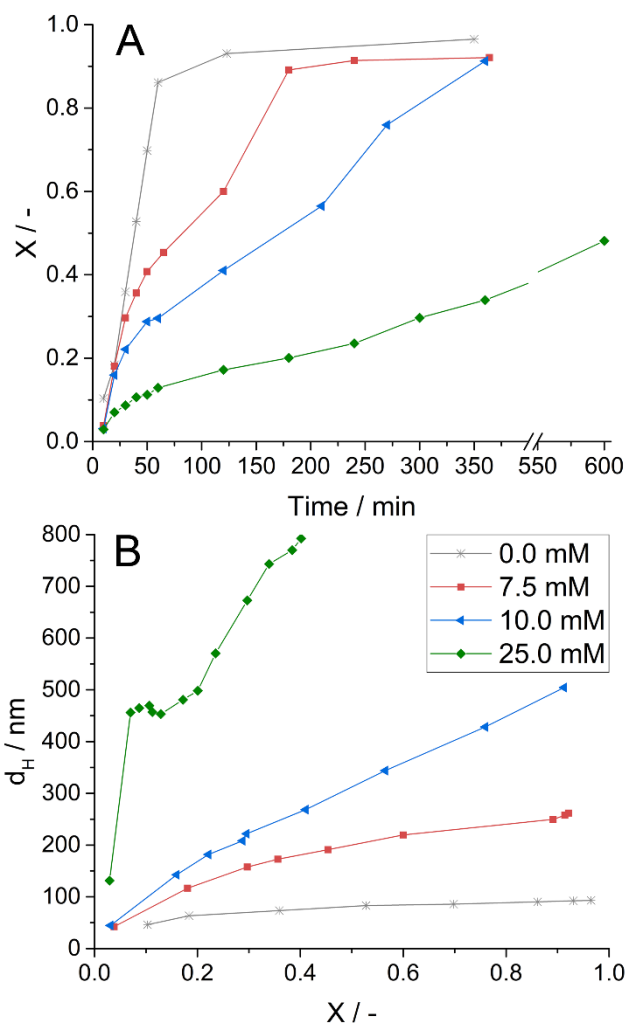


Figure 5. a) Evolution of monomer conversion (X) with time and b) hydrodynamic diameter (d_H) with X for the emulsion polymerizations conducted at 0.0, 7.5, 10.0 and 25.0 mM [NaCl]. [KPS] = 0.25 mM.

calculate the rate of polymerization (R_p) in an emulsion polymerization reaction is introduced:⁴¹

$$(1.2) \quad R_p = \frac{dX}{dt} \frac{\text{mol}_M}{V_W} = \frac{N_p}{V_W} k_p C_{p,M} \bar{n}$$

where mol_M is the initial moles of monomer, V_W is the total volume of water, k_p is the propagation rate coefficient of the monomer, $C_{p,M}$ is the concentration of the monomer within the latex particles, N_p is the number of latex particles, \bar{n} is the average number of radicals per particle and N_A is the Avogadro number.

The reactions with [NaCl] = 0.0 – 10.0 mM started at similar rate of polymerization, that is proportional to dX/dt in Figure 5A. The reason for this is that N_p is initially the same in all the reactions and equal to the number of nanogels introduced. In fact, previously we hypothesized that in the early stages of the reaction styrene polymerizes within the nanogels and phase-separates on the side forming a small Janus-like primary particle.²⁶ This type of behavior was also observed in the case of seeded emulsion polymerizations using crosslinked seed

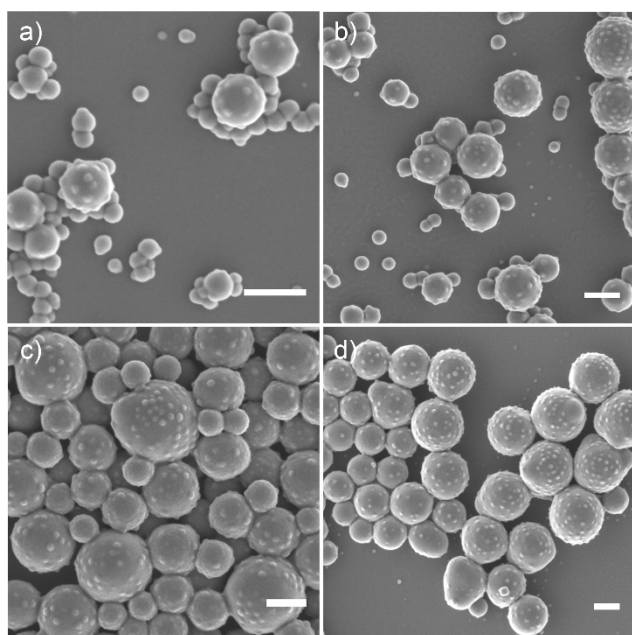


Figure 6. SEM analysis of the samples taken at a) 24 min ($X = 0.14$), b) 40 min ($X = 0.33$), c) 120 min ($X = 0.67$) and d) 150 min ($X = 0.89$) during the emulsion polymerization of styrene conducted in the presence of nanogels and $[\text{NaCl}] = 7.5$ mM. Scale bars: 200 nm.

particles.^{23,46} When no background electrolyte was added, the nanogel high, unscreened charge can keep these growing Janus particles colloidally stable. In this case, R_p stayed relatively constant throughout the reaction, which reached *ca.* 90% conversion within the first hour (Figure 5A). Instead, in the case of $[\text{NaCl}] = 7.5$ and 10.0 mM, at about 15/20% conversion, R_p decreased noticeably. The suppression of the rate of reaction upon salt addition in emulsion polymerization was described in the literature to be linked to an increase in coagulative nucleation events, which form a lower number of stable particles.^{8,12,29} The same mechanism would explain how bigger particles bearing multiple nanogels on their surface are formed (Figures 3-4 and S4). Here it is similarly expected that upon growth of a soft polystyrene lobe off a nanogel particle, the partial screened charge, κ^{-1} *ca.* 9 and 2-3 nm respectively for $[\text{NaCl}] = 0.0$ mM and $[\text{NaCl}] = 7.5$ -10.0 mM (Table 2), it is not capable of granting colloidal stability and the nanogels cluster to decrease their surface energy. Samples taken during the reaction carried out at $[\text{NaCl}] = 7.5$ mM and analyzed *via* SEM confirmed that indeed this is the case (Figure 6). 24 min after the beginning of the reaction the system consisted of a mixture of unreacted nanogels, Janus nanogel-poly(styrene) precursors and a series of particles characterized by varying nanogel coverage and size. This also showed that the sample is of broad distribution from the very beginning of the reaction, which is not unexpected as clustering of Janus particles typically yields a broad mixture of products.⁴⁶⁻⁴⁸ In this process, in the first stages of the reaction the latex particles can be formed by clusters of Janus precursors or nanogel clusters. This progressively decreases the concentration of available nanogels and results in a decreased patch density for particles formed in later stages of the reaction.

As the reaction conducted at $[\text{NaCl}] = 7.5$ mM progressed, at 120 min a portion of the more densely covered particles appeared deformed (Figure 6C). Interestingly, the extent of the deformation increased in the last stages of the reaction (Figures 6D and 4C). It is still not entirely clear what is the cause of such deformation and why this was not observed at higher $[\text{NaCl}]$. The first possible explanation is that newly formed growing particles which lose colloidal stability can coalesce with bigger, more densely covered latexes. Alternatively, the effect could be explained as phase separation from a partially crosslinked latex. The nanogels still bearing reactive double bonds²⁶ could act as crosslinking points between the polymer chains making the shell of the latex partially crosslinked. As more poly(styrene) is formed, this would phase separate on the side of the latex as its radial growth is partially constrained.⁴⁶ In the case of the reactions carried out at higher $[\text{NaCl}]$, the higher nanogel coverage on the surface would create a more densely crosslinked shell, which would hinder the phase separation process.

The reaction carried out at 25.0 mM NaCl continued the trend observed in the previous experiments whilst including some additional interesting features. As shown in Figure 5B, clusters of about 450 nm in diameter were formed rapidly in the first stages of the reaction, at $X < 0.1$. Note that the data points reported in Figure 5B are intensity-based average values. A more careful look at the DLS volume-based distribution of the samples taken at this stage of the reaction clearly displayed the rapid formation of such objects (Figure S5). Interestingly, the clusters were not detected at time 0, after the system was heated up, in presence of monomer, but before initiator addition. Here it is argued that these clusters may be monomer droplets highly covered in nanogels. This would also infer that the adopted nanogels can act as emulsifiers only once they become (lightly) amphiphilic.

For $[\text{NaCl}] = 25.0$ mM the formation of a significant lower number of particles came with a drastic lowering of R_p ; X was *ca.* 50% after 10h. Using equation 5.4, R_p was found to be $1.7 \times 10^{-2} \text{ mol s}^{-1} \text{ dm}^{-3}$ for $[\text{NaCl}] = 0.0$ mM and 2.7×10^{-3} , 1.9×10^{-3} and $4.8 \times 10^{-4} \text{ mol s}^{-1} \text{ dm}^{-3}$ respectively for $[\text{NaCl}] = 7.5$, 10.0 and 25.0 mM after clustering (measured between 60 and 120 min). This drop in R_p is only partially explained in terms of reduction of N_p , as it is counteracted by a much greater average number of radical per particles (\bar{n}) that typically occurs in large latex particles.⁴¹ In fact, while small latex particles tend to obey the so-called zero-one kinetic, where $\bar{n} = 0.5$, large particles follow a pseudo-bulk mechanism where \bar{n} can reach much greater values.⁴¹ Detailed interpretation of \bar{n} calculations is complicated for broad particle size distributions. Generically, we can state that for a fixed monomer-to-water ratio the larger the particles, the more compartmentalization is faded out, which manifests itself in a reduced overall rate of polymerization.

The reaction conducted at $[\text{NaCl}] = 25.0$ mM (and at the same total ionic strength but at higher initiator concentration) led to the formation of what essentially appeared to be core-shell

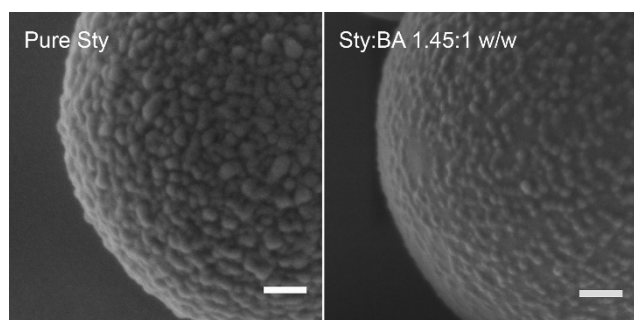


Figure 7. Close-up on a latex particle made of pure poly(styrene) (left) or poly(styrene)-*co*-poly(*n*-butyl acrylate) (right); [NaCl] = 25.0 mM, [KPS] = 0.25 mM. Scale bars: 100 nm.

particles where a polystyrene core was surrounded by a dense shell of nanogels (Figures 4 and S4). In these reactions styrene was used as monomer mainly because its high glass transition temperature (T_g) aids electron microscopy analysis. However, these polymerizations could also be conducted using lower T_g monomers, such as *n*-butyl acrylate. In particular a reaction was carried out using a 1.45:1 w:w styrene (Sty):*n*-butyl acrylate (BA) mixture in a way of synthesizing film forming latexes, which upon drying would form a film characterized by a honeycomb substructure of stabilizing particles within a polymeric matrix.²¹ This type of latexes are rather interesting as it has previously been shown that the resulting films can show improved tack adhesion⁴⁹ and mechanical^{25,50} properties with respect to the fully homogenous equivalent. Interestingly, SEM analysis of the latexes formed in the presence of increasing amounts of BA revealed an apparent lower nanogel coverage on the latex surface with respect to the reactions carried out with pure styrene (Figure 7). This is likely related to the softer nature of BA-rich particles, where the nanogels are more embedded within the surface. Additionally, it is known that in styrene-BA copolymerizations BA-rich polymeric chains, which are likely to reside on the particle surface, are produced towards the end of the reaction.⁵¹ On the contrary, chains produced during the rest of the polymerization will be richer in styrene. This has interesting implications on the properties of the final latex. In fact, the T_g of this latex was measured to be equal to 41°C and 35°C respectively *via* dynamic mechanical analysis (DMA, Figure S6) and differential scanning calorimetry (DSC, Figure S7). In comparison, the estimated glass transition temperature (T_g) of the homogenous copolymer according to the Fox equation⁵² would have been 16°C. For this reason, films with a good degree of transparency were obtained only when casting latex suspensions on glass slides and drying them at 50–70°C (Figure 8). When the same was attempted at lower temperature (40°C) the films presented substantially higher opacity suggesting incomplete coalescence of the latex particles, and the presence of air voids in the film (Figure S8).⁵³

Conclusions

We showed that the effect that a background electrolyte, in this work NaCl, plays on a nanogel stabilized Pickering emulsion

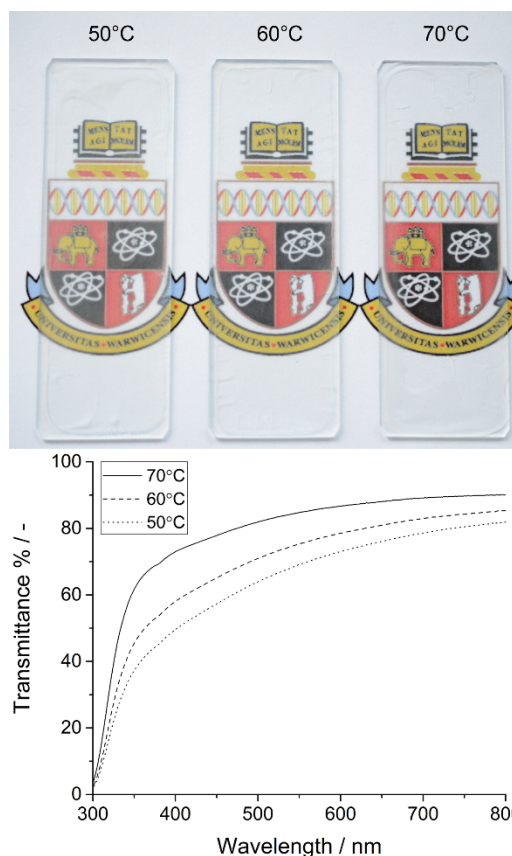


Figure 8. (Top) Polymer films obtained from casting a latex suspension on glass slides and drying at 50–70°C. (Bottom) UV-Vis spectra of the films.

polymerization process, is substantial. It was observed that overall it is possible to fabricate a range of latexes characterized by varied size distribution and patch density by simply tailoring the salt concentration in the dispersing medium.

We believe that the Janus latexes made in absence of salt open up an interesting route towards functionalized anisotropic particles as the nanogels can be made from a variety of monomers. The particles with multiple patches show on average a broad particle size distribution. Whereas for model colloids this may not be desired, for more practical applications in the area of adhesives and coatings broad particle distribution aids low viscosity, high solid systems. The armored latexes with a dense layer of nanogels form an interesting class of particles of core-shell type morphology. We illustrated this briefly with films made from “soft” armored latexes. Such materials can find application into polymeric films where an intricate substructure of stabilizing agent is present. This not only solves the problem of surfactant migration in polymer films,^{1,54} but it also has the advantage of combining the properties of the two different phases involved.

Experimental section

Materials

Styrene ($\geq 99\%$) and *n*-butyl acrylate ($\geq 99\%$) were purchased from Sigma Aldrich and filtered through activated basic

aluminum oxide prior to use to remove the inhibitors. Potassium persulfate (KPS) ($\geq 99.0\%$), sodium chloride ($\geq 99.5\%$), sodium benzoate ($\geq 99.0\%$) were purchased from Sigma Aldrich and used as received.

Equipment and methods

Average hydrodynamic diameters and distributions were measured by dynamic light scattering (DLS) on a Malvern Zetasizer Nano ZS operating at 25°C and at a detection angle of 173°. ζ -potential measurements on latexes were carried out at 1.0 wt% polymer in aq. [NaCl] at pH 8.8 using disposable folded cuvettes (Malvern). Scanning electron microscopy (SEM) images were collected on a ZEISS Gemini SEM or a FEI Nova NanoSEM 450 FEGSEM. Samples were diluted in deionized water and casted on a silicon wafer fragment, which had been adhered to an aluminum stab using conductive copper tape. The samples prepared in this way were carbon or chromium coated before imaging. Film formation studies were carried out by casting 2.0 \pm 0.1 ml of latex suspension on a glass slide. The film was left to dry in an oven at varied temperatures overnight. Dynamic mechanical analysis (DMA) was performed on a PerkinElmer DMA 8000. DMA analysis was carried out on a 9.8 \times 7.5 \times 1.1 mm polymer film which was formed by casting multiple layers of the Sty/BA = 1.45:1 w:w latex suspension on a poly(propylene) pan, allowing each layer to dry overnight at 70°C. The final thickness was 1.1 mm. The sample for DMA analysis was heated at 5°C/min from -50°C to 150°C under N₂ at 1.00 Hz frequency and with a static force of 2.00 N. Differential scanning calorimetry (DSC) analysis was carried out on the same specimen on a Mettler-Toledo DSC1. The sample was heated and cooled twice at 10°C/min from 0°C to 120°C under N₂. UV-Vis spectra were recorded on an Agilent technologies Cary 60 UV-Vis. Spectra were recorded on the polymer films casted on glass slides positioned at a 90° angle with respect to the incident beam.

Nanogel stabilized emulsion polymerizations

In a typical emulsion polymerization experiment an aqueous dispersion of nanogels (3.50 g, 13.0 wt% aq. suspension) was diluted with aq. NaCl (154.5 g). The pH of the suspension was adjusted to 8.8 using aq. NaOH 1.0 M. The reaction mixture was charged in a sealed 250 ml round bottom flask equipped with an oval stirrer bar and it was purged with nitrogen for 30 min. Next, styrene (15.95 g, ca. 17.5 ml), which had been previously purged with nitrogen for 30 min, was injected into the reactor using a degassed syringe. The system was heated up to 75°C. The reaction was started upon injection of an aqueous KPS solution (1.5 ml, 6.9 mg/ml) and was allowed to fully react overnight. When the kinetic of the reaction was monitored, samples (typically 1 g) were withdrawn throughout the polymerization to check monomer conversion *via* gravimetry. Kinetic experiments were monitored for 6-10 hours but the reactions were left to react overnight (total reaction time = 20-24h).

Capillary hydrodynamic fractionation (CHDF)

Particle size distributions were measured by capillary hydrodynamic fractionation (CHDF) using a CHDF 2000 (Matec Applied Sciences) instrument equipped with a Waters 486 UV detector ($\lambda = 200$ nm). A proprietary surfactant mixture (GR500) in DI water was used as eluent. The eluent was composed of a polyoxyethylene-based non-ionic surfactant (1.0 g/L), sodium dodecyl sulfate (29 mg/L) and sodium azide (0.5 mg/L). The eluent was filtered through a 0.2 μ m filter before use. The flow rate was set at 1.3 ml/min and the column operated at 30°C and 4000 psi. Latex samples (ca. 9-10 wt% in water) were diluted 1:8.3 times in the eluent mixture prior to injection. The injection of the latex in the instrument was followed by the one of sodium benzoate (0.2 wt% in eluent), used as a flowrate marker.

Conflicts of interest

There are no conflicts to declare.

Acknowledgements

The Australian paint company Dulux Australia is acknowledged for financial funding (AL). We would like to thank the Royal Society of Chemistry for awarding AL a Researcher Mobility Grant to support a collaboration between Warwick and Monash University. Simon Peake (Yates Australia) is acknowledged for the great help in carrying out CHDF analysis. Dr. Brooke W. Longbottom is thanked for the help in collecting the SEM image in Figure 2A.

Notes and references

- 1 S. Jiang, A. Van Dyk, A. Maurice, J. Bohling, D. Fasano and S. Brownell, *Chem. Soc. Rev.*, 2017, **46**, 3792–3807.
- 2 C. Pichot, T. Delair and A. Elaissari, in *Polymeric Dispersions: Principles and Applications*, Springer Netherlands, Dordrecht, 1995, pp. 515–539.
- 3 R. Jovanović and M. A. Dubé, *J. Macromol. Sci. Part C Polym. Rev.*, 2004, **44**, 1–51.
- 4 T. Wang and J. L. Keddie, *Adv. Colloid Interface Sci.*, 2009, **147–148**, 319–332.
- 5 A. K. Van Der Vegt, *From polymers to plastics*, VSSD, Delft, 2006.
- 6 A. Snezhko, I. S. Aranson, N. Becker, T. Proslie, A. Demortière and M. V. Sapozhnikov, *Nat. Commun.*, 2014, **5**, 1–7.
- 7 M. Chen, M. Z. Mokhtar, E. Whittaker, Q. Lian, B. Hamilton, P. O'Brien, M. Zhu, Z. Cui, S. A. Haque and B. R. Saunders, *Nanoscale*, 2017, **9**, 10126–10137.
- 8 J. W. Goodwin, R. H. Ottewill, R. Pelton, G. Vianello and D. E. Yates, *Br. Polym. J.*, 1978, **10**, 173–180.
- 9 N. J. Warren and S. P. Armes, *J. Am. Chem. Soc.*, 2014, **136**, 10174–10185.
- 10 R. M. Fitch, *Polym. React. Eng.*, 2003, **11**, 911–953.
- 11 R. M. Fitch, *Polymer Colloids: A Comprehensive introduction*, Academic Press, London, 1997.
- 12 J. W. Goodwin, J. Hearn, C. C. Ho and R. H. Ottewill, *Br.*

- Polym. J.*, 1973, **5**, 347–362.
- 13 F. J. Schork, Y. Luo, W. Smulders, J. P. Russum, A. Butté and K. Fontenot, in *Advances in Polymer Science*, 2005, vol. 175, pp. 129–255.
- 14 P. J. Colver, C. A. L. Colard and S. A. F. Bon, *J. Am. Chem. Soc.*, 2008, **130**, 16850–16851.
- 15 L. A. Fielding, J. Tonnar and S. P. Armes, *Langmuir*, 2011, **27**, 11129–11144.
- 16 C. A. L. Colard, R. F. A. Teixeira and S. A. F. Bon, *Langmuir*, 2010, **26**, 7915–7921.
- 17 A. Lotierzo and S. A. F. Bon, *Polym. Chem.*, 2017, **8**, 5100–5111.
- 18 R. F. A. Teixeira, H. S. McKenzie, A. A. Boyd and S. A. F. Bon, *Macromolecules*, 2011, **44**, 7415–7422.
- 19 N. Sheibat-Othman, A. M. Cenacchi-Pereira, A. M. Dos Santos and E. Bourgeat-Lami, *J. Polym. Sci. Part A Polym. Chem.*, 2011, **49**, 4771–4784.
- 20 B. Brunier, N. Sheibat-Othman, Y. Chevalier and E. Bourgeat-Lami, *Langmuir*, 2016, **32**, 112–124.
- 21 J. L. Keddie, E. Bourgeat-Lami, F. Dalmas, K. L. Elidottir, S. J. Hinder, I. Martín-Fabiani, M. Lansalot, M. L. Koh and I. Jurewicz, *ACS Appl. Nano Mater.*, 2018, **1**, 3956–3968.
- 22 A. Walther, M. Hoffmann and A. H. E. Müller, *Angew. Chemie - Int. Ed.*, 2008, **47**, 711–714.
- 23 B. T. T. Pham, C. H. Such and B. S. Hawkett, *Polym. Chem.*, 2015, **6**, 426–435.
- 24 S. C. Thickett and P. B. Zetterlund, *ACS Macro Lett.*, 2013, **2**, 630–634.
- 25 E. Limousin, N. Ballard and J. M. Asua, *Polym. Chem.*, 2019, **10**, 1823–1831.
- 26 A. Lotierzo, B. W. Longbottom, W. H. Lee and S. A. F. Bon, *ACS Nano*, 2019, **13**, 399–407.
- 27 D. C. Blackley and A. R. D. Sebastian, *Br. Polym. J.*, 1989, **21**, 313–326.
- 28 A. S. Dunn and Z. F. M. Said, *Polymer (Guildf.)*, 1982, **23**, 1172–1176.
- 29 M. E. Dobrowolska and G. J. M. Koper, *Soft Matter*, 2014, **10**, 1151–1154.
- 30 J. L. Mateo and I. Cohen, *J. Polym. Sci. Part A*, 1964, **2**, 711–730.
- 31 W. M. Thomas, E. H. Gleason and G. Mino, *J. Polym. Sci.*, 1957, **24**, 43–56.
- 32 T. Guha and S. R. Palit, *J. Polym. Sci. Part A Gen. Pap.*, 1963, **1**, 877–893.
- 33 P. A. Lovell and M. S. El-Aasser, *Emulsion Polymerization and Emulsion Polymers*, J. Wiley, 1997.
- 34 R. Pelton, PhD Thesis, University of Bristol, 1976.
- 35 S. A. F. Bon and P. J. Colver, *Langmuir*, 2007, **23**, 8316–8322.
- 36 S. Cauvin, P. J. Colver and S. A. F. Bon, *Macromolecules*, 2005, **38**, 7887–7889.
- 37 P. C. Hiemenz and R. Rajagopalan, *Principles of Colloid and Surface Chemistry*, Taylor and Francis Group, 1997.
- 38 H. Ohshima, in *Electrical Phenomena at Interfaces and Biointerfaces*, John Wiley & Sons, Inc., Hoboken, NJ, USA, 2012, pp. 27–34.
- 39 S. Kawaguchi, A. Yekta and M. A. Winnik, *J. Colloid Interface Sci.*, 1995, **176**, 362–369.
- 40 A. Katchalsky and P. Spitnik, *J. Polym. Sci.*, 1947, **2**, 432–446.
- 41 R. G. Gilbert, *Emulsion polymerization, a mechanistic approach.*, Academic Press Inc., San Diego, 1995.
- 42 C. M. Miller, J. Venkatesan, C. A. Silebi, E. D. Sudol and M. S. El-Aasser, *J. Colloid Interface Sci.*, 1994, **162**, 11–18.
- 43 C. A. Silebi and J. G. Dosramos, *J. Colloid Interface Sci.*, 1989, **130**, 14–24.
- 44 J. G. DosRamos and C. A. Silebi, *J. Colloid Interface Sci.*, 1990, **135**, 165–177.
- 45 R. B. Bird, W. E. Stewart and E. N. Lightfoot, *Transport Phenomena*, John Wiley & Sons, Inc, New York, 2nd editio., 2007.
- 46 H. R. Sheu, M. S. El-Aasser and J. W. Vanderhoff, *J. Polym. Sci. Part A Polym. Chem.*, 1990, **28**, 629–651.
- 47 T. S. Skelhon, Y. Chen and S. A. F. Bon, *Soft Matter*, 2014, **10**, 7730–7735.
- 48 D. J. Kraft, W. S. Vlug, C. M. Van Kats, A. Van Blaaderen, A. Imhof and W. K. Kegel, *J. Am. Chem. Soc.*, 2009, **131**, 1182–1186.
- 49 T. Wang, P. J. Colver, S. A. F. Bon and J. L. Keddie, *Soft Matter*, 2009, **5**, 3842–3849.
- 50 X. Zhou, H. Shao and H. Liu, *Colloid Polym. Sci.*, 2013, **291**, 1181–1190.
- 51 F. Ziaee and M. Nekoomanesh, *Polymer (Guildf.)*, 1998, **39**, 203–207.
- 52 P. C. Hiemenz and T. P. Lodge, *Polymer Chemistry*, Taylor and Francis Group, 2nd ed., 2007.
- 53 P. A. Steward, J. Hearn and M. C. Wilkinson, *Adv. Colloid Interface Sci.*, 2000, **86**, 195–267.
- 54 D. Scalarone, M. Lazzari, V. Castelvetro and O. Chiantore, *Chem. Mater.*, 2007, **19**, 6107–6113.